Hybrid Solar Cells with Polymer/Fullerene Bulk Heterojunction Layers Containing *in-situ* Synthesized CdS Nanocrystals

Eunjoo Kwak[1] · Sungho Woo[1,2] · Hwajeong Kim[1,3] · Youngkyoo Kim[1]*

[1]Organic Nanoelectronics Laboratory, School of Applied Chemical Engineering, Kyungpook National University, Daegu 702-701, Republic of Korea
[2]Energy Research Division, Daegu Gyeongbuk Institute of Science and Technology (DGIST), Daegu 711-873, Republic of Korea
[3]Research Institute of Advanced Energy Technology, Kyungpook National University, Daegu 702-701, Republic of Korea

ABSTRACT: We report hybrid solar cells fabricated with polymer/fullerene bulk heterojunction layers that contain inorganic nanocrystals synthesized by *in-situ* reaction in the presence of polymer chains. The inorganic (cadmium sulfide) nanocrystal (CdS_{NC}) was generated by the reaction of cadmium acetate and sulfur by varying the reaction time up to 30 min. The synthesized CdS_{NC} showed a rectangular flake shape, while the size of CdS_{NC} reached ca. 150 nm when the reaction time was 10 min. The performance of hybrid solar cells with CdS_{NC} synthesized for 10 min was better than that of a control device, whereas poor performances were measured for other hybrid solar cells with CdS_{NC} synthesized for more than 10 min.

Key words: Hybrid solar cells, Bulk heterojunction, CdS nanocrystal, *In-situ* synthesis

Nomenclature

CdS_{NP} : Cadmium sulfide nanocrystal
J_{SC} : Short circuit current density, mA/cm^2
V_{OC} : Open circuit voltage, V
FF : Fill factor, %
PCE : Power conversion efficiency, %
R_S : Series resistance, $k\Omega \cdot cm^2$
R_{SH} : Shunt resistance, $k\Omega \cdot cm^2$

1. Introduction

Polymer solar cells with single active (light-absorbing) layers, which feature bulk heterojunction (BHJ) structures, have recently attracted considerable attention because of their potentials for flexible and lightweight plastic solar modules[1-4]. In particular, polymer solar cells can be fabricated by employing continuous roll-to-roll coating processes at low temperatures (<150°C), which are far lower than the fabrication temperatures for conventional inorganic solar cells. Therefore, polymer solar cells are expected to contribute to the realization of low-cost ultrathin plastic film-type solar modules like a wall paper[5,6].

*Corresponding author: ykimm@knu.ac.kr
Received November 3, 2014; Revised November 6, 2014; Accepted November 6, 2014

However, the stability of polymer solar cells becomes a bottleneck for commercialization, even though the power conversion efficiency has recently reached 9~11%[7-18]. Of various factors affecting the stability and lifetime of polymer solar cells, the morphological instability of BHJ layers is understood to lead to the gradually degraded device performances[13,14]. One of the morphological instability can be attributed to the nanoscopic phase segregation between polymer chains and fullerene molecules and/or the chemical reaction among fullerene molecules. In this regard, it is considered as one of good approaches to introduce inorganic nanoparticles or nanocrystals instead of fullerene derivatives[19-25].

In this work, we introduced cadmium sulfide (CdS) nanocrystals (CdS_{NC}) to the BHJ layer, which is composed of poly (3-hexylthiophene) (P3HT) and phenyl-C_{61}-butyric acid methyl ester ($PC_{61}BM$), by employing an *in-situ* reaction of precursor materials. The resulting CdS nanocrystals showed rectangular shapes with various aspect ratios, while their size reached ~200 nm. The device performances were investigated by varying the reaction time compared to the control device without the CdS nanocrystals.

2. Experimental

To synthesize CdS_{NC}, the co-solvent of 8 ml dichlorobenzene (DCB, Sigma-Aldrich, anhydrous, 99%) and 4 ml dimethyl

sulfoxide (DMSO, Sigma-Aldrich, analytical grade) was charged into a three-necked flask and heated up to 100°C. Then cadmium acetate dihydrate ($Cd(Ac)_2$, Sigma-Aldrich, powder, 98%) and P3HT (P3HT, Rieke Metals, weight-average molecular weight = 50 kDa, polydispersity index = 2, regioregularity > 98%) were dissolved in the co-solvent (P3HT:$Cd(Ac)_2$ = 10:1 by weight). Sulfur (20 mg) was added to another flask charged with DCB at 100°C and heated up to 180°C for complete dissolution. The sulfur-dissolved DCB solution was quickly added to the P3HT/$Cd(Ac)_2$-dissolved solution. This solution was heated up to 180°C and kept for 30 min for reaction (see scheme 1). The reaction was terminated by adding methanol (anhydrous), followed by removal of solvents and remained starting materials by employing centrifugation and extraction. The CdS_{NC}/P3HT mixture was dried in a vacuum oven. Finally, the ternary solution (P3HT:CdS_{NC}:$PC_{61}BM$ = 45:5:50 by weight) was prepared by mixing the CdS_{NC}/P3HT mixture and $PC_{61}BM$ in DCB.

$$Cd(Ac)_2 \cdot 2H_2O + S + P3HT \xrightarrow[180\ ^oC]{DMSO + DCB} CdS_{NC} + P3HT + CO_2 + H_2O$$

Scheme 1. *In-situ* synthesis of CdS_{NC} from its precursor, $Cd(Ac)_2$, in the mixture solution containing P3HT. Three different reaction times (10 min, 20 min, 30 min) were applied

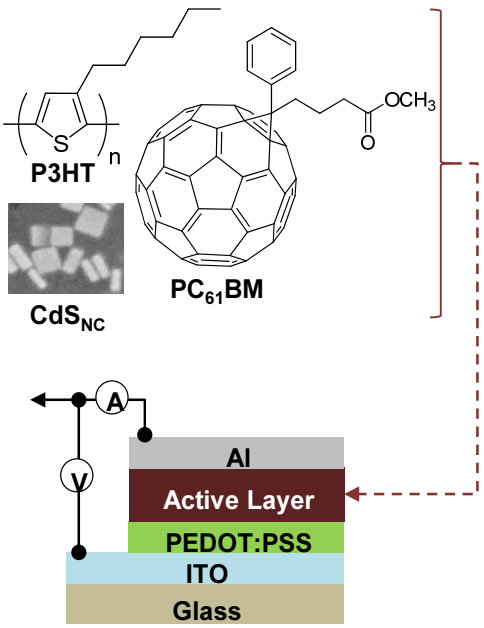

Fig. 1. Illustration for the device structure and the materials used for the active layer. Note that the SEM image for CdS_{NC} was taken from Fig. 2

For the fabrication of solar cells, glass substrates coated with the indium-tin oxide (ITO) layer were subject to photolithography/etching processes in order to make bottom electrodes (see Fig. 1). On top of the patterned ITO-glass substrates, poly (3,4-ethylenedioxythiophene): poly (styrenesulfonate) (PEDOT:PSS, Clevios PH500, 40 nm) was spin-coated and thermally annealed at 230°C for 15 min. Next, the hybrid bulk heterojunction layers (P3HT:CdS_{NC}:$PC_{61}BM$) were coated on the PEDOT:PSS layers and soft-baked at 60°C for 30 min. These samples were transferred to a vacuum chamber and the Al electrodes (80 nm) were deposited by thermal evaporation. Finally, the fabricated devices were thermally annealed at 150°C for 30 min. All devices were kept inside an argon-filled glove box before measurement.

The morphology of the hybrid bulk heterojunction films was measured using a scanning electron microscope (HD-2300, Hitachi). The performance of solar cells was measured using a specialized solar cell measurement system equipped with a solar simulator (Model 92250, Newport-Oriel) and an electrometer (Model 2400, Keithley). The intensity of the simulated solar light was fixed as 100 mW/cm^2 (air mass (AM) 1.5G).

3. Results and Discussion

As shown in Fig. 2, the CdS_{NC} synthesized in the presence of P3HT showed rectangular flake shapes with the maximum size (longest axis) of ca. 150 nm. Considering the flake-like shapes of CdS_{NC}, it is considered that most of the CdS_{NC} flakes in the hybrid film may locate with their wider faces parallel to the film

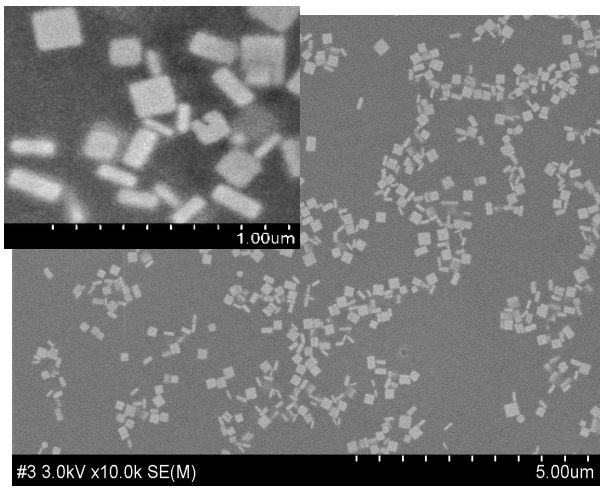

Fig. 2. SEM image for the film prepared from the CdS_{NC}/P3HT mixture (reaction time: 10 min): The left-top image shows the SEM image measured with a higher magnification

plane. However, the size of CdS_{NC} became bigger (>500 nm) when the reaction time was increased more up to 30 min (images are not shown here).

Fig. 3(a) shows the current density-voltage (J-V) curves of devices with the P3HT:CdS_{NP}:$PC_{61}BM$ BHJ layer. A control device (CD), which has the P3HT:$PC_{61}BM$ BHJ layer (without CdS_{NC}), exhibited relatively good performance. Interestingly, the device with the hybrid BHJ layer, which contains the CdS_{NC} component synthesized for 10 min, showed better performance than the control device. However, poor performances were obtained for the devices with the hybrid BHJ layers containing the CdS_{NC} component synthesized for 20 min and 30 min. The reason can be found from the dark J-V curves (Fig. 3(b)), which deliver the charge transport characteristics for each device. Looking at the dark current density at a higher forward bias, we find that the lower dark current density was measured for the devices with the hybrid BHJ layers containing the CdS_{NC} component synthesized for 20 min and 30 min. Hence it is supposed that the charge transport might be suppressed owing to the coarse morphology by the presence of large CdS_{NC} components in the case of long reaction times (20 min and 30 min).

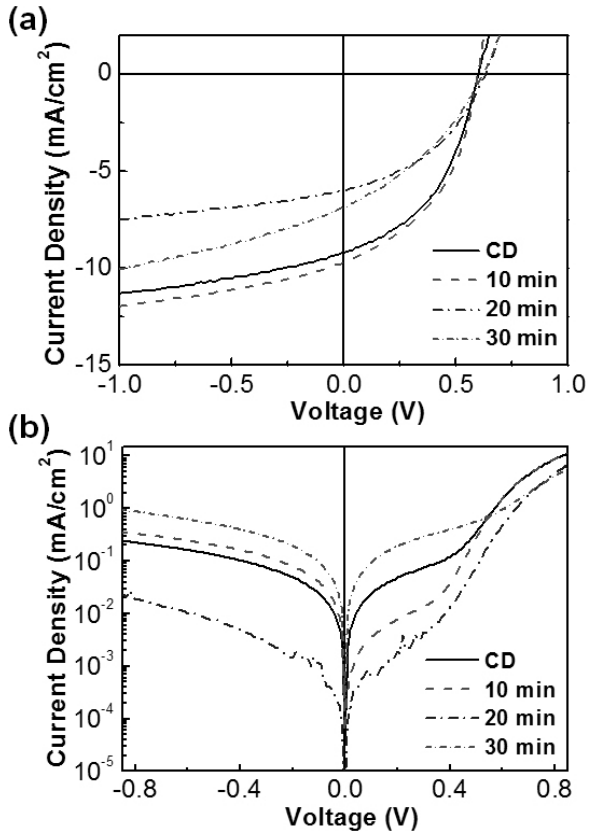

Fig. 3. (a) Light J-V curves of devices under illumination of a simulated solar light (AM 1.5G, 100 mW/cm^2). (b) Dark J-V curves of devices. The reaction time for the *in-situ* synthesis of CdS_{NC} is given on each graph

Here we need to understand the role of CdS_{NC} in the BHJ layer because the better device performance was obtained for the hybrid device with the CdS_{NC} component synthesized for 10 min. As illustrated in Fig. 3(b), the CdS_{NC} component might play an electron-acceptor role together with the $PC_{61}BM$ component when it comes to the conduction band (3.6 eV) of CdS_{NC}[26]. After charge separation between P3HT and CdS_{NC}, the electrons in the CdS_{NC} component could undergo fast charge transport due to the highly ordered crystal features of CdS_{NC} component. In addition, the light scattering by the presence of CdS_{NC} in the BHJ layer is considered to contribute to the light harvesting leading to the increased short circuit current density (J_{SC}). Considering the conduction band of CdS_{NC}, the open circuit voltage (V_{OC}) could not be lowered by the presence of CdS_{NC}. As a consequence, the power conversion efficiency (PCE) of the hybrid device with the CdS_{NC} component synthesized for 10 min reached 2.6%, which is slightly higher than the PCE (2.4%) of the control device.

4. Conclusions

The CdS nanocrystals (CdS_{NC}) were *in-situ* synthesized from their precursors in the mixture solution that contains P3HT polymers. The synthesized CdS_{NC} showed a rectangular flake shape with a maximum size of less than 150 nm. The ternary

Table 1. Summary of solar cell performances according to the reaction time for CdS_{NC}. The series resistance (R_S) was calculated at around open circuit voltages in the light J-V curves, while the shunt resistance (R_{SH}) was calculated at around short circuit current densities in the light J-V curves. 'CD' denotes the control device with the binary BHJ layer (P3HT:$PC_{61}BM$) without CdS_{NC}

Devices	J_{SC} (mA/cm^2)	V_{OC} (V)	FF (%)	PCE (%)	R_S (kΩ•cm^2)	R_{SH} (kΩ•cm^2)
CD	9.2	0.59	45.3	2.46	0.23	3.6
10 min	9.7	0.59	45.4	2.60	0.17	2.2
20 min	6.0	0.62	41.6	1.55	0.42	7.9
30 min	6.9	0.62	35.0	1.50	0.48	3.7

blend solutions were prepared by adding $PC_{61}BM$ to the CdS_{NC}/P3HT mixture, which were used as a BHJ layer for hybrid solar cells. The hybrid solar cells with the CdS_{NC} synthesized for 10 min exhibited better performances than the control device, which was attributed to the improved charge transport through the CdS_{NC} component in the BHJ layer and the enhanced light-harvesting by the light scattering caused by the CdS_{NC} component. However, longer reaction times led to the poor device performances.

Acknowledgments

This work was supported by the Korean government grants (Basic Science Research Program_2009-0093819, NRF_2012K1 A3A1A09027883, MOTIE_10048434, Basic Research Laboratory Program_2011-0020264, NRF_2012R1A1B3000523), DGIST R&D Program of the Ministry of Science, ICT and Future Planning of Korea (14-EN-03).

References

1. Y. Huang, E. J. Kramer, A. J. Heeger, G. C. Bazan. "Bulk heterojunction solar cells: morphology and performance relationships", Chem. Rev., Vol. 114, pp. 7006-7043, 2014.
2. S. E. Shaheen, C. J. Brabec, N. S. Sariciftci, "2.5% efficient organic plastic solar cells", Appl. Phys. Lett., Vol. 78, No. 6, pp. 841, 2001.
3. Y. Kim, S. Cook, S. M. Tuladhar, S. A. Choulis, J. Nelson, J. R. Durrant, D. D. C. Bradley, M. Giles, I. McCulloch, C. S. Ha, M. Ree, "A strong regioregularity effect in self-organizing conjugated polymer films and high-efficiency polythiophene: fullerene solar cells", Nat. Mater., Vol. 5, No. 3, pp. 197-203, 2006.
4. H. Kim, S. Nam, J. Jeong, S. Lee, J. Seo, H. Han, Y. Kim, "Organic solar cells based on conjugated polymers : History and recent advances", Korean J. Chem. Eng., Vol. 31, No. 7, pp. 1095-1104, 2014.
5. F. C. Krebs, S. A. Gevorgyan, J. Alstrup, "A roll-to-roll process to flexible polymer solar cells: model studies, manufacture and operational stability studies", J. Mater. Chem., Vol. 19, pp. 5442-5451, 2009.
6. S. Lee, S. Nam, J. Seo, J. Jeong, H. Kim, S. Woo, Y. Kim, "Polymer solar cells with micrometer-scale engraved active nanolayers fabricated by pressing with metal molds", Energy Technol., Vol. 2, pp. 731-720, 2014.
7. W. Li, A. Furlan, K. H. Hendriks, M. M. Wienk, R. A. J. Janssen, "Efficient tandem and triple-junction polymer solar cells", J. Am. Chem. Soc., Vol. 135, pp. 5529-5532, 2013.
8. Z. C. He, C. M. Zhong, S. J. Su, M. Xu, H. B. Wu, Y. Cao, "Enhanced power-conversion efficiency in polymer solar cells using an inverted device structure", Nat. Photonics, Vol. 6, pp. 591-595, 2012.
9. S. Woo, W. H. Kim, H. Kim, Y. Yi, H. -K. Lyu, Y. Kim, "8.9% single-stack inverted polymer solar cells with electron-rich polymer nanolayer-modified inorganic electron-collecting buffer layers", Adv. Energy Mater., Vol. 4, pp. 1301692, 2014.
10. J. You, C.-C. Chen, Z. Hong, K. Yoshimura, K. Ohya, R. Xu, S. Ye, J. Gao, G. Li, Y. Yang, "10.2% power conversion efficiency polymer tandem solar cells consisting of two identical sub-cells", Adv. Mater., Vol. 25, pp. 3973-3978, 2003.
11. E. Zimmermann, P. Ehrenreich, T. Pfadler, J. A. Dorman, J. Weickert, L. Schmidt-Mende, "Erroneous efficiency reports harm organic solar cell research", Nat. Photonics, Vol. 8, pp. 669-672, 2014.
12. M. O. Reese, S. A. Gevorgyan, M. Jørgensen, E. Bundgaard, S. R. Kurtz, D. S. Ginley, D. C. Olson, M. T. Lloyda, P. Morvillo, E. A. Katz, A. Elschner, O. Haillant, T. R. Currier, V. Shrotriya, M. Hermenau, M. Riede, K. R. Kirov, G. Trimmel, T. Rath, O. Inganäs, F. Zhang, M. Andersson, K. Tvingstedt, M. Lira-Cantu, D. Laird, C. McGuiness,S. Gowrisanker, M. Pannone, M. Xiao, J. Hauch, R. Steim, "Consensus stability testing protocols for organic photovoltaic materials and devices", Sol. Energy Mater. Sol. Cells, Vol. 95, pp. 1253-1267, 2011.
13. H. Kim, M. Shin, J. Park, Y. Kim, "Initial performance changes of polymer/fullerene solar cells by short-time exposure to simulated solar light", ChemSusChem, Vol. 3, pp. 476-486, 2010.
14. S. Lee, S. Nam, H. Lee, H. Kim, Y. Kim, "Device performance and lifetime of polymer:fullerene solar cells with UV-ozone-irradiated hole-collecting buffer layers", ChemSusChem, Vol. 4, pp. 1607-1612, 2011.
15. H. C. Wong, Z. Li, C. H. Tan, H. Zhong, Z. Huang, H. Bronstein, I. McCulloch, J. T. Cabral, J. R. Durrant, "Morphological stability and performance of polymer-fullerene solar cells under thermal stress: the impact of photoinduced PC60BM oligomerization", ACS Nano, Vol. 8, pp. 1297-1308, 2014.
16. H. Kim, S. Nam, H. Lee, S. Woo, C. -S. Ha, M. Ree, Y. Kim, "Influence of controlled acidity of hole-collecting buffer layers on the performance and lifetime of polymer:fullerene solar cells", J. Phys. Chem. C, Vol. 115, pp. 13502-13510, 2011.
17. M. Jørgensen, K. Norrman, S. A. Gevorgyan, T. Tromholt, B. Andreasen, F. C. Krebs, "Stability of polymer solar cells", Adv. Mater., Vol. 24, pp. 580-612, 2012.
18. F. C. Krebs, H. Spanggaard, "Significant improvement of polymer solar cell stability", Chem. Mater., Vol. 17, pp. 5235–5237, 2005.
19. J. Kim, S. Lee, S. Nam, H. Lee, H. Kim, Y. Kim, "A pronounced dispersion effect of crystalline silicon nanoparticles on the performance and stability of polymer:fullerene solar cells", ACS Appl. Mater. Interfaces, Vol. 4, pp. 5300-5308, 2012.
20. S. Shao, K. Zheng, K. Zidek, P. Chabera, T. Pullerits, F. Zhang, "Optimizing ZnO nanoparticle surface for bulk heterojunction hybrid solar cells", Sol. Energy Mater. Sol. Cells, Vol. 118, pp. 43-47, 2013.

21. E. K. Park, J. H. Kim, I. A. Ji, H. M. Choi, J. H. Kim, K. T. Lim, J. H. Bang, Y. S. Kim, "Optimization of CdSe quantum dot concentration in P3HT:PCBM layer for the improved performance of hybrid solar cells", Microelectron. Eng., Vol. 119, pp. 169-173, 2014.
22. S. Nam, J. Kim, H. Kim, Y. Kim, "Effect of film thickness in hybrid polymer/polymer solar cells with zinc oxide nanoparticles", J. Nanosci. Nanotechnol., Vol. 11, pp. 5733-5736, 2011.
23. J. Kim, S. Nam, J. Jeong, H. Kim, Y. Kim, "Effect of silicon-nanoparticle addition on the nanostructure of polythiophene: fullerene bulk heterojunction solar cells", J. Korean Phys. Soc., Vol. 61, pp. 434-438, 2012.
24. Z. Liu, Y. Sun, J. Yuan, H. Wei, X. Huang, L. Han, W. Wang, H. Wang, W. Ma, "High-efficiency hybrid solar cells based on polymer/PbSxSe1-x nanocrystals benefiting from vertical phase segregation", Adv. Mater., Vol. 25, pp. 5772-5778, 2013.
25. S. Woo, S. Lee, Y. S. Han, H. Lyu, K. Kim, H. Kim, Y. Kim, "Hybrid solar cells based on bulk heterojunction films of conjugated polymers and single crystalline Si nanowires", J. Nanoelectron. Optoelectron., Vol. 5, pp. 139-142, 2010.
26. M. Li, J. C. Li, "Size effects on the band-gap of semiconductor compounds", Mater. Lett., Vol. 60, pp. 2526-2529, 2006.